Formation and Deprotonation Kinetics of the Sitting-Atop Complex of Copper(II) Ion with 5,10,15,20-Tetraphenylporphyrin Relevant to the Porphyrin Metalation Mechanism. Structure of Copper(II)−Pyridine Complexes in Acetonitrile As Determined by EXAFS Spectroscopy

Yasuhiro Inada, Yumi Sugimoto, Yuko Nakano, Yuki Itoh, and Shigenobu Funahashi*

Laboratory of Analytical Chemistry, Faculty of Science, Nagoya University, Nagoya 464-8602, Japan

Received April 13, 1998

The formation of a sitting-atop (SAT) complex of Cu(II) ion with 5,10,15,20-tetraphenylporphyrin (H_2tpp) in acetonitrile has been observed, and the kinetic parameters for the formation were determined as follows: $k_{S0} = (3.6 \pm 0.1) \times 10^5$ mol^{-1} dm^3 s^{-1} at 25.0 °C, $\Delta H_{S0}^{\ddagger} = 56 \pm 5$ kJ mol^{-1}, and $\Delta S_{S0}^{\ddagger} = 46 \pm 19$ J mol^{-1} K^{-1}. The ^{1}H NMR spectrum of the SAT complex ($Cu(H_2tpp)^{2+}$) indicated that two pyrrolenine nitrogens coordinate to the Cu(II) ion and that two protons bound to the pyrrole nitrogens remain. The protons were abstracted by the addition of pyridine (py) as the Brønsted base to give the Cu(tpp) metalloporphyrin. In the presence of py, the product for the reaction of the Cu(II) ion with H_2tpp was Cu(tpp) instead of the SAT complex. The observed conditional rates for the formation of $Cu(H_2tpp)^{2+}$ and Cu(tpp) were interpreted by the contribution of Cu^{2+}, $Cu(py)^{2+}$, and $Cu(py)_2^{2+}$ species, and the second-order rate constants of the SAT complex formation were $k_{S1} = (3.5 \pm 0.3) \times 10^4$ mol^{-1} dm^3 s^{-1} for $Cu(py)^{2+}$ and $k_{S2} = 90 \pm 2$ mol^{-1} dm^3 s^{-1} for $Cu(py)_2^{2+}$. Deprotonation rates were measured by following the reaction between the SAT complex and py as a function of the py concentration, and the second-order rate constant was determined to be $(2.3 \pm 0.1) \times 10^2$ mol^{-1} dm^3 s^{-1}. The present kinetic results have indicated that the SAT complex exists during the course of the metalation process and that the SAT complex formation is a rate-determining step.

Introduction

Many metalloporphyrins and analogues, such as hemoglobin, myoglobin, and chlorophyll, play significant roles in vivo.[1−3] The function of these metalloporphyrins occurs at the axial site of an incorporated metal ion, and the majority of studies on the metalloporphyrin focus on the axial site.[4] On the other hand, the metalloporphyrin formation reaction is also one of the most important processes in biological systems, and the importance has been pointed out in relation to the biosynthesis of heme.[3−9] The metalloporphyrin formation mechanism is not, however, well established, not only in biological systems but also in simple systems in vitro.[10] In 1960, Fleisher and Wang proposed that an intermediate should exist in the metalation process,[11] and this intermediate was called a sitting-atop (SAT) complex, in which two pyrrolenine nitrogens coordinate to the metal ion and two protons on the pyrrole nitrogens still remain. The existence of the SAT complex could explain the experimental kinetics of the metalation for several porphyrins in *N*,*N*-dimethylformamide (DMF),[12−15] acetic acid,[16] dimethyl sulfoxide (DMSO),[17] and H_2O.[18,19] However, whereas the formation constant of the SAT complex was reported as being on the order of 10^2-10^4 mol^{-1} dm^3 for Cu(II) and Zn(II) ions in DMF,[12,14] the fast reaction corresponding to the formation of the SAT complex was not observed. Furthermore, the reports on the detection of the SAT complex have been very limited, only in peculiar systems,[20−23] and kinetic investigations of the SAT complex formation have never been examined.

The metalloporphyrin formation (reaction 1) between a metal ion (M^{n+}) and a general porphyrin (H_2p) certainly proceeds by multiple steps. At least two steps, i.e., the coordination of the

(1) da Silva, J. J. R. F.; Williams, R. J. P. *The Biological Chemistry of the Elements*; Clarendon Press: Oxford, 1991.
(2) Fenton, D. E. *Biocoordination Chemistry*; Oxford Science Publications: Oxford, 1995.
(3) Lavallee, D. K. *Mol. Struct. Energ.* **1988**, *9*, 279.
(4) *The Porphyrins*; Dolphin, D., Ed.; Academic Press: New York, 1978; Vols. VI and VII.
(5) Blackwood, M. E., Jr.; Rush, T. S., III; Medlock, A.; Dailey, H. A.; Spiro, T. G. *J. Am. Chem. Soc.* **1997**, *119*, 12170.
(6) Lloyd, S. G.; Franco, R.; Moura, J. J. G.; Moura, I.; Ferreira, G. C.; Huynh, B. H. *J. Am. Chem. Soc.* **1996**, *118*, 9892.
(7) Conn, M. M.; Prudent, J. R.; Schultz, P. G. *J. Am. Chem. Soc.* **1996**, *118*, 7012.
(8) Taketani, S. In *Regulation of Heme Protein Synthesis*; Fujita, H., Ed.; AlphaMed Press: OH, 1994.
(9) Dailey, H. A. *Biosynthesis of Heme and Chlorophylls*; McGraw-Hill: New York, 1990.
(10) Lavallee, D. K. *The Chemistry and Biochemistry of N-Substituted Porphyrins*; VCH: New York, 1987.
(11) Fleischer, E. B.; Wang, J. H. *J. Am. Chem. Soc.* **1960**, *82*, 3498.
(12) Funahashi, S.; Yamaguchi, Y.; Tanaka, M. *Bull. Chem. Soc. Jpn.* **1984**, *57*, 204.
(13) Funahashi, S.; Yamaguchi, Y.; Tanaka, M. *Inorg. Chem.* **1984**, *23*, 2249.
(14) Robinson, L. R.; Hambright, P. *Inorg. Chim. Acta* **1991**, *185*, 17.
(15) B.-Ackerman, M. J.; Lavallee, D. K. *Inorg. Chem.* **1979**, *18*, 3358.
(16) Funahashi, S.; Saito, K.; Tanaka, M. *Bull. Chem. Soc. Jpn.* **1981**, *54*, 2695.
(17) Pasternack, R. F.; Vogel, G. C.; Skowronek, C. A.; Harris, R. K.; Miller, J. G. *Inorg. Chem.* **1981**, *20*, 3763.
(18) Hambright, P.; Chock, P. B. *J. Am. Chem. Soc.* **1974**, *96*, 3123.
(19) Turay, J.; Hambright, P. *Inorg. Chem.* **1980**, *19*, 562.
(20) Fleischer, E. B.; Dixon, F. *Bioinorg. Chem.* **1977**, *7*, 129.
(21) Burnham, B. F.; Zuckerman, J. J. *J. Am. Chem. Soc.* **1970**, *92*, 1547.
(22) Letts, K.; Mackay, R. A. *Inorg. Chem.* **1975**, *14*, 2993.
(23) Macquet, J. P.; Theophanides, T. *Can. J. Chem.* **1973**, *51*, 219.

10.1021/ic980420d CCC: $15.00
Published on Web 09/18/1998

$$M^{n+} + H_2p \rightleftharpoons M(p)^{(n-2)+} + 2H^+ \quad (1)$$

pyrrolenine nitrogens to M^{n+} and the deprotonation of the pyrrole proton should be involved in the overall process of reaction 1. According to previous kinetic experiments,[12−19] however, the apparent reaction proceeded in a single step. To elucidate the metalation mechanism, kinetic observation for each step is needed. Prevention of the deprotonation of the pyrrole protons will be achieved by the appropriate selection of solvents with low Brønsted basicity, because released protons cannot be stabilized in such a solvent. In general, we must use noncharged metal species such as MX_n (X = halogenide) as a source of metal ions, because a solvent with low basicity cannot solvate the free metal ion. The use of such metal species, however, leads to complexity in the mechanistic analysis of the metalation reaction. The conflict concerning the selection of solvent and metal was overcome by the use of acetonitrile (AN) in this work.

The basicity of AN is much lower than that of other aprotic solvents, such as DMF, DMSO, and pyridine (py).[24−26] On the other hand, it is well-known that AN is a good solvent for the metal salts, such as $M(ClO_4)_n$ and $M(CF_3SO_3)_n$, though its donating ability is not so great.[27] Thus, the use of AN is the best selection for the mechanistic investigation of the metalation reaction.[28] In this work, we performed kinetic measurements between the Cu(II) ion and H_2tpp in AN and first succeeded in detecting directly the SAT complex and evaluating independently its formation and deprotonation kinetics. First of all, equilibria and structures of Cu(II) complexes in the presence of py in AN were characterized in order to determine the initial state for the reaction systems subsequently investigated.

Experimental Section

Materials. A small excess of CF_3SO_3H was dropped into suspended CuO (Wako, 99.99%) in water. The solution was stirred for a day, residues were filtered, and the resultant solution was then concentrated to obtain blue crystals of $Cu(H_2O)_6(CF_3SO_3)_2$. The containing water was completely expelled by heating at 300 °C, and a white powder of $Cu(CF_3SO_3)_2$ was obtained. Anal. Found: Cu, 17.6%. Calcd for $Cu(CF_3SO_3)_2$: Cu, 17.6%.

Pyridine (Wako, Pr. G.) was distilled twice under nitrogen atmosphere after dehydration using 4A molecular sieves. H_2tpp (Dojin) was used without further purification, because it was spectrophotometrically confirmed that the existence of impurities, such as 5,10,15,20-tetraphenylchlorine, was negligible. 5,10,15,20-Tetraphenylporphyrinatocopper(II) (Cu(tpp)) was synthesized according to a reported procedure.[29,30] Acetonitrile was dried over 4A molecular sieves and distilled under nitrogen. Sample solutions were prepared by dissolving each reagent in AN under a nitrogen atmosphere in order to prevent contamination by water in air. The content of water in the sample solutions was confirmed to be less than 5×10^{-3} mol kg^{-1} by the Karl−Fisher method. Although all the measurements were carried out under a nitrogen atmosphere, we confirmed that water less than 10^{-2} mol dm^{-3} did not affect any results.

Spectrophotometric Titration. To determine the formation constants of Cu(II)−py complexes in AN, spectrophotometric titrations were performed. The measurement apparatus consisted of an automatic buret (E665, Metrohm), a glass titration vessel, a flow cell (light path = 1 cm), a Teflon coated diaphragm pump (E-30, Kyoritsu), and a UV−vis spectrophotometer (UV-265FW, Shimadzu). The Cu(II) ion solution was titrated with a py solution, and the absorption spectra for each titration point were recorded after achieving equilibrium. The obtained absorbance data were analyzed by the least-squares calculation using the program MQSPEC over the wavelength range 500−850 nm.[31]

EXAFS Measurements. The sample solutions for the extended X-ray absorption fine structure (EXAFS) measurements were absorbed in porous glass disks, which were sealed in a polyethylene bag in order to prevent moisture ingress and evaporation of AN. X-ray absorption spectra were measured in the vicinity of the Cu K-edge using the BL-10B station at the Photon Factory of the National Laboratory for High Energy Physics.[32,33] The white synchrotron radiation was monochromatized by a Si(311) channel-cut crystal. The incident and transmitted X-ray intensities were simultaneously measured by an ionization chamber with a length of 17 and 31 cm, filled with N_2 gas and a 3:17 mixture of Ar and N_2 gas, respectively.

The details of EXAFS data analysis were previously reported.[34,35] The model function of EXAFS oscillation $\chi_{calc}(k)$ is given as[36−41]

$$\chi_{calc}(k) = \sum_j \left\{ \frac{N_j}{kr_j^2} \right\} F_j(\pi,k) \sin\{2kr_j - \alpha_j(k)\} \exp\left(-2\sigma_j^2 k^2 - \frac{2r_j}{\lambda} \right) \quad (2)$$

where $F_j(\pi,k)$ is the backscattering amplitude from each of N_j scatterers j at a distance r_j from the Cu center. σ_j is the Debye−Waller factor, λ is the mean free path of an ejected photoelectron, and $\alpha_j(k)$ is the total phase shift. The values of $F_j(\pi,k)$ and $\alpha_j(k)$ reported by McKale et al. were used.[42] The parameters E_0 and λ were determined by an EXAFS spectrum of an aqueous solution of Cu(II) ion as a standard sample on the basis of the structure parameters determined by the X-ray diffraction method.[43,44] The obtained values of E_0 and λ were kept constant during the course of the structural analysis of the other sample solutions, and the values of r_j, σ_j, and N_j, were optimized as variables. The least-squares calculations for refinement of the structure parameters were applied to the Fourier filtered $k^3\chi(k)$ values so as to minimize the error-squares sum, $\sum\{k^3\chi_{obsd}(k) - k^3\chi_{calc}(k)\}^2$. Calculations were performed using the program REX (Rigaku).[45]

NMR Measurements. ^{1}H NMR spectra for sample solutions were measured using an AMX400 FT-NMR spectrometer (Bruker) at 400.13 MHz and 21 ± 1 °C for the following sample solutions: (1) 4.0×10^{-2} mol dm^{-3} of H_2tpp in $CDCl_3$, (2) 1.0×10^{-4} mol dm^{-3} of H_2tpp

(24) Barrette, W. C., Jr.; Johnson, H. W., Jr.; Sawyer, D. T. *Anal. Chem.* **1984**, *56*, 1890.
(25) Izutsu, K. *Acid−Base Dissociation Constants in Dipolar Aprotic Solvents*; Blackwell Scientific Publication: London, 1990.
(26) Lias, S. G.; Liebman, J. F.; Levin, R. D. *J. Phys. Chem. Ref. Data* **1984**, *13*, 695.
(27) Gutmann, V. *The Donor−Acceptor Approach to Molecular Interactions*; Plenum Press: New York, 1978.
(28) Although the solubility of H_2tpp is quite low in AN, the high molar absorptivity of H_2tpp in the visible region permitted runs of metalation reactions.
(29) Dorough, G. D.; Miller, J. R.; Huennekens, F. M. *J. Am. Chem. Soc.* **1951**, *73*, 4315.
(30) Adler, A. D.; Longo, F. R.; Kampas, F.; Kim, J. *J. Inorg. Nucl. Chem.* **1970**, *32*, 2443.
(31) Suzuki, H.; Ishiguro, S. *Inorg. Chem.* **1992**, *31*, 4178.
(32) Nomura, M. *KEK Report 85-7*; National Laboratory for High Energy Physics: Tsukuba, 1985.
(33) Nomura, M.; Koyama, A. *KEK Report 89-16*; National Laboratory for High Energy Physics: Tsukuba, 1989.
(34) Inada, Y.; Sugimoto, K.; Ozutsumi, K.; Funahashi, S. *Inorg. Chem.* **1994**, *33*, 1875.
(35) Inada, Y.; Ozutsumi, K.; Funahashi, S.; Soyama, S.; Kawashima, T.; Tanaka, M. *Inorg. Chem.* **1993**, *32*, 3010.
(36) Sayers, D. E.; Stern, E. A.; Lytle, F. W. *Phys. Rev. Lett.* **1971**, *27*, 1204.
(37) Stern, E. A. *Phys. Rev. B* **1974**, *10*, 3027.
(38) Lytle, F. W.; Sayers, D. E.; Stern, E. A. *Phys. Rev. B* **1975**, *11*, 4825.
(39) Stern, E. A.; Sayers, D. E.; Lytle, F. W. *Phys. Rev. B* **1975**, *11*, 4836.
(40) Lengeler, B.; Eisenberger, P. *Phys. Rev. B* **1980**, *21*, 4507.
(41) Lee, P. A.; Citrin, P. H.; Eisenberger, P.; Kincaid, B. M. *Rev. Mod. Phys.* **1981**, *53*, 769.
(42) McKale, A. G.; Veal, B. W.; Paulikas, A. P.; Chan, S. K.; Knapp, G. S. *J. Am. Chem. Soc.* **1988**, *110*, 3763.
(43) Ohtaki, H.; Radnai, T. *Chem. Rev.* **1993**, *93*, 115.
(44) Marcus, Y. *Chem. Rev.* **1988**, *88*, 1475.
(45) Teranishi, T.; Harada, M.; Asakura, K.; Asanuma, H.; Saito, Y.; Toshima, N. *J. Chem. Phys.* **1994**, *98*, 7967.

Table 1. Experimental Conditions for EXAFS Measurements

sample	solvent	C_{Cu} mol dm^{-3}	C_{py} mol dm^{-3}	mole fraction				
				Cu^{2+}	$Cu(py)^{2+}$	$Cu(py)_2^{2+}$	$Cu(py)_3^{2+}$	$Cu(py)_4^{2+}$
W	H_2O	0.482		1.00	0	0	0	0
P0	AN	0.498	0	1.00	0	0	0	0
P1	AN	0.498	0.303	0.46	0.48	0.06	0	0
P2	AN	0.498	0.919	0.01	0.21	0.72	0.06	0
P3	AN	0.498	1.21	0	0.02	0.55	0.41	0.02
P4	AN	0.498	1.69	0	0	0.04	0.53	0.43
P5	AN	0.498	2.21	0	0	0	0.01	0.99

in CD_3CN, and (3) a CD_3CN solution containing 7.0×10^{-3} mol dm^{-3} of H_2tpp and 3.5×10^{-2} mol dm^{-3} of Cu^{2+}.

Kinetic Measurements. Absorption spectra were recorded on a UV−vis spectrophotometer (UV-265FW), and the spectral changes for the fast reactions were followed by a stopped-flow rapid-detection system (RSP-600-06, Unisoku). The absorbance changes for the reaction between the Cu(II) ion and H_2tpp were monitored at 416 nm. A stopped-flow three-sample mixer (newly developed and now commercially available RS-3, Unisoku) with three sample syringes and two mixing chambers was used for the kinetic measurements of the deprotonation reaction; after a first mixing of AN solutions of the Cu(II) ion and H_2tpp, the absorbance changes at 414 nm for the deprotonation were followed by a subsequent mixing of the first mixed solution and a py solution.

Results and Discussion

Equilibria and Structures of Pyridine Complexes of Cu(II) Ion in Acetonitrile. The Cu(II) ion solutions (the initial concentration = 2.45×10^{-2} and 4.51×10^{-3} mol dm^{-3}) were titrated with the py solutions of 0.544 and 0.551 mol dm^{-3}, respectively. An example of the titration curve at 700 nm is shown in Figure S1A (S: Supporting Information). The observed spectral data were analyzed by the least-squares calculation on the basis of eq 3

$$A_i = \sum_{n=0}^{4} \epsilon_{Cu(py)_n^{2+},i}[Cu(py)_n^{2+}] \quad (3)$$

where A_i is the absorbance at wavelength i and $\epsilon_{Cu(py)_n^{2+},i}$ is the molar absorption coefficient of $Cu(py)_n^{2+}$ at wavelength i. The total concentrations of the Cu(II) ion (C_{Cu}) and py (C_{py}) are described by eq 4 using the formation constant β_n of the Cu(II)−py complexes defined as $\beta_n = [Cu(py)_n^{2+}][Cu^{2+}]^{-1}[py]^{-n}$.

$$C_{Cu} = [Cu^{2+}] + \sum_{n=1}^{4} \beta_n[Cu^{2+}][py]^n,$$

$$C_{py} = [py] + \sum_{n=1}^{4} n\beta_n[Cu^{2+}][py]^n \quad (4)$$

The obtained absorption spectra of the $Cu(py)_n^{2+}$ species are shown in Figure S1B, and the values of β_n at 25.0 ± 0.1 °C are as follows: $\log(\beta_1/\text{mol}^{-1}\text{ dm}^3) = 6.4 \pm 0.5$, $\log(\beta_2/\text{mol}^{-2}\text{ dm}^6) = 11.9 \pm 0.6$, $\log(\beta_3/\text{mol}^{-3}\text{ dm}^9) = 15.8 \pm 0.6$, and $\log(\beta_4/\text{mol}^{-4}\text{ dm}^{12}) = 18.5 \pm 0.6$. In water, the corresponding values were reported as 2.60, 4.54, 5.80, and 6.70, respectively.[46] It is reasonable that the formation constants in AN are much larger than those in water due to the weaker solvation of AN for the Cu(II) ion. This is consistent with the negative value (−55.3 kJ mol^{-1}) of the transfer free energy of Cu^{2+} from AN to water.[47] We have used the β_n values in order to calculate the distribution of the species in the sample solutions containing py.

(46) Sun, M. S.; Brewer, D. G. *Can. J. Chem.* **1967**, *45*, 2429.
(47) Cox, B. G.; Parker, A. J.; Waghome, W. E. *J. Phys. Chem.* **1974**, *78*, 1731.

Table 2. Structure Parameters of the Cu(II)−py Complexes in Acetonitrile[a]

	Cu−N(an)$_{eq}$[b]		Cu−N(py)$_{eq}$[c]		Cu−N(an)$_{ax}$[d]	
	N	r/pm[e]	N	r/pm[e]	N	r/pm[e]
$Cu(an)_6^{2+}$	4	199			2	218
$Cu(py)(an)_5^{2+}$	3	202	1	199	2	230
$Cu(py)_2(an)_4^{2+}$	2	202	2	202	2	230
$Cu(py)_3(an)_3^{2+}$	1	205	3	202	2	232
$Cu(py)_4(an)_2^{2+}$			4	204	2	237

[a] $E_0 = 9002.6 \pm 0.3$ eV, $\lambda = 594 \pm 19$ pm. [b] The σ value of 5.9 pm, which was obtained from the data of sample P0, was used for all samples. [c] The σ value of 5.8 pm, which was obtained from the data of sample P5, was used for all samples. [d] The σ values were 16.7, 15.8, 13.8, 13.2, and 11.1 pm for $Cu(an)_6^{2+}$, $Cu(py)(an)_5^{2+}$, $Cu(py)_2(an)_4^{2+}$, $Cu(py)_3(an)_3^{2+}$, and $Cu(py)_4(an)_2^{2+}$, respectively. [e] Error of r is estimated to be ca. 1 pm.

The values of C_{Cu} and C_{py} of the sample solutions for the EXAFS measurements and the calculated mole fraction of each Cu(II)−py complex are summarized in Table 1. The observed EXAFS oscillations $\chi_{obs}(k)$ weighted by k^3 and the Fourier transforms are shown in Figures S2 and S3, respectively. The main peaks (ca. 160 pm) in Figure S3 were attributed to the nearest Cu−N or Cu−O interactions. In AN, the longer Cu···C nonbonding interactions appeared in the r range 200−300 pm, where the multiple scatterings would also be included. In the case of the sample solutions containing py, the peaks originating from the nonbonding Cu···C(py) interactions and the multiple scatterings were also observed around 300−400 pm. The intensities of these peaks gradually increased with respect to an increase in C_{py}. In this work, the main peaks ($85 < r/\text{pm} < 205$ in Figure S3) were extracted and used for the structural analysis. The Fourier filtered and the calculated EXAFS oscillations are consistent with each other, as shown in Figure S4, and the obtained structure parameters are summarized in Table 2.

For the structural analysis of the Cu(II)−py complexes, the structure parameters around the Cu center of Cu^{2+} and $Cu(py)_4^{2+}$ were first determined from the data of samples P0 and P5 (see Table 1), respectively. Because sample P1 contained both Cu^{2+} and $Cu(py)^{2+}$, the contribution of $Cu(py)^{2+}$ to the $k^3\chi_{obs}(k)$ function was extracted using the Fourier filtered $k^3\chi(k)$ values of sample P0 on the basis of mole fractions. The structure parameters of $Cu(py)_3^{2+}$ were similarly determined from the data of samples P4 and P5. In the case of samples P2 and P3, the r values for three kinds of interaction, i.e., Cu−N(an)$_{eq}$ (the nitrogen of AN in the equatorial site), Cu−N(py)$_{eq}$ (the nitrogen of py in the equatorial site), and Cu−N(an)$_{ax}$ (the nitrogen of AN in the axial site), and the σ value for the Cu−N(an)$_{ax}$ interaction were optimized by fixing the N values for all interactions and the σ values for Cu−N(an)$_{eq}$ and Cu−N(py)$_{eq}$. Because the obtained r values of samples P2 and P3 were accepted as the mean values of some Cu(II)−py species ($Cu(py)^{2+}$ and $Cu(py)_2^{2+}$ for sample P2; $Cu(py)_2^{2+}$ and $Cu(py)_3^{2+}$ for sample P3), the structure parameters of $Cu(py)_2^{2+}$

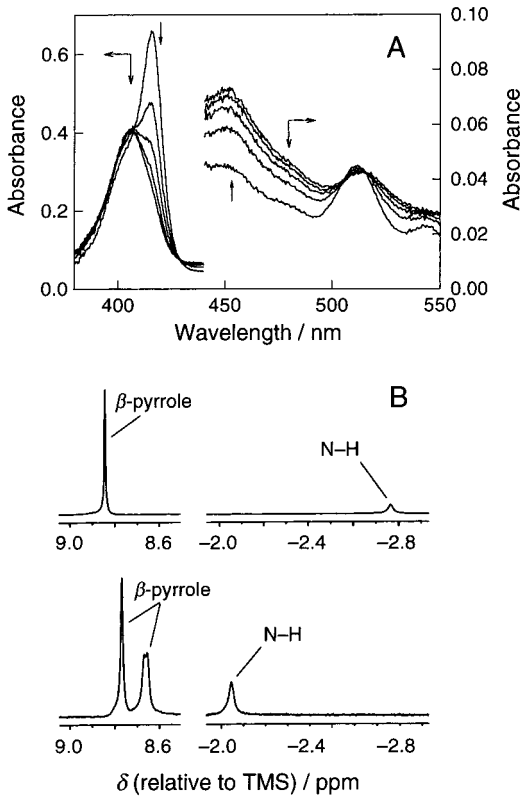

Figure 1. Spectral change for the formation of the SAT complex (A) and ^{1}H NMR spectra for H_2tpp and the SAT complex (B): (A) the spectra at 10.4, 20.4, 30.4, 40.4, and 60.4 ms after the start of the reaction, $[H_2tpp]_0 = 1.5 \times 10^{-6}$ mol dm^{-3}, $[Cu^{2+}] = 5.47 \times 10^{-4}$ mol dm^{-3}, and 25.0 ± 0.1 °C; (B) the peaks of the N−H (higher field) and β-pyrrole protons (lower field) for H_2tpp (upper, 4.0×10^{-2} mol dm^{-3} of H_2tpp in $CDCl_3$) and the SAT complex (lower, CD_3CN solution containing 7.0×10^{-3} mol dm^{-3} of H_2tpp and 3.5×10^{-2} mol dm^{-3} of Cu^{2+}).

were determined on the basis of mole fractions, and they were in agreement with each other within the experimental uncertainties.

The r value of the Cu−N(py)$_{eq}$ interaction in Cu(py)$_4^{2+}$ was consistent with the mean value (204.6 pm) of the Cu−N bond lengths of Cu(py)$_4$ (OCOCF$_3$)$_2$ in a single crystal[48] and was by 5 pm longer than that of the Cu−N(an)$_{eq}$ of Cu^{2+} in AN. The longer M−N bond lengths in pyridine derivatives compared to those in AN were also reported for Mn(II) and Ni(II) ions.[49−51] The fact that a gradual increase in r was observed with respect to an increase in the number of py molecules around the Cu center for both the Cu−N(an)$_{eq}$ and Cu−N(py)$_{eq}$ interactions reflects the stronger σ-donation of py compared to that of AN.

Characterization of the SAT Complex in Acetonitrile. Figure 1A shows the spectral change for the reaction between Cu^{2+} and H_2tpp in AN. This process was completed within ca. 100 ms even in an excess Cu^{2+} concentration of the order of 10^{-4} mol dm^{-3} and was extremely fast in comparison with the usual metalloporphyrin formation of the Cu(II) ion.[12,15,17,19] The absorption spectrum of the product (λ_{max} = 406 nm) is apparently different from those of H_2tpp (λ_{max} = 417 nm) and Cu(tpp) (λ_{max} = 414 nm) and has a characteristic broader Soret band compared with those of H_2tpp and Cu(tpp). This fact suggests that the porphyrin ring in the product should be distorted. According to the ^{1}H NMR results described just below, in addition to the above results, we have concluded that the product of the reaction between Cu^{2+} and H_2tpp is the SAT complex (Cu(H_2tpp)$^{2+}$), which is stable at least for a few hours in AN.

Figure 1B shows ^{1}H NMR peaks assigned to N−H and β-pyrrole protons for H_2tpp in $CDCl_3$ and the SAT complex in CD_3CN, and the chemical shift values are summarized in Table 3 together with the reported values for H_2tpp.[52,53] Although the SAT complex contains the paramagnetic Cu(II) ion having S =1/2, the β-pyrrole protons have been clearly observed as seen in some low-spin Fe(III)−porphyrin complexes.[54,55] The ^{1}H NMR spectra of H_2tpp in $CDCl_3$ and CD_3CN were almost identical, and the signals of the N−H and β-pyrrole protons were observed at a ratio of 1:4 in intensity. The finding that the signal of the N−H protons in the SAT complex was clearly observed at −2.05 ppm relative to TMS strongly indicated that the N−H protons remain in the SAT complex (Cu(H_2tpp)$^{2+}$). In contrast to the case of H_2tpp, two kinds of β-protons for the SAT complex were observed with a ratio of 1:1, which had twice the area of the peak for N−H protons. The peaks, one a singlet and the other a doublet, were attributed to the protons in the pyrrolenine group coordinated and in the pyrrole group not coordinated to the Cu(II) ion, respectively. A similar splitting was reported for H_2tpp at the low temperature of −80 °C, because the N−H tautomerism at such a low temperature was frozen,[52,53] where the signal of the β-pyrrole protons of the pyrrole groups with N−H protons was observed at a lower field relative to that of the pyrrolenine groups without the N−H protons (see Table 3). The opposite trend in chemical shift was, however, observed for the SAT complex, i.e., the doublet peak assigned to the β-pyrrole protons appears at a higher field (see Figure 1B). This indicates that the two pyrrolenine nitrogens without an N−H proton bind to the paramagnetic Cu(II) ion, because the dipole−dipole and scalar coupling interactions with the paramagnetic ion lead to their downfield shift.[56,57] Furthermore, the peak for N−H protons was shifted downfield relative to that of H_2tpp. This is ascribed to both the distortion of the porphyrin ring and the dipole−dipole interaction with the paramagnetic ion. Because the N−H protons in H_2tpp are highly shifted to the upper field due to the ring current of the planar porphyrin ring, the distortion of the porphyrin ring in the SAT complex then leads to the downfield shift. Two types of porphine skeletons (**1** and **2** in Chart 1) are possible for the SAT complex with pyrrolenine nitrogens coordinating to the Cu(II) ion. The observed ^{1}H NMR spectrum determines the symmetrical structure of **1**, because in the case of **2** the two β-protons of the pyrrolenine ring are not identical. Furthermore, the clear splitting of two kinds of β-protons indicates that the N−H tautomerism in the SAT complex is not so fast with respect to the time scale of the ^{1}H NMR measurements at 21 ± 1 °C.

(48) Pradilla, S. J.; Chen, H. W.; Koknat, F. W.; Fackler, J. P., Jr. *Inorg. Chem.* **1979**, *18*, 3523.
(49) Kurihara, M.; Ozutsumi, K.; Kawashima, T. *J. Sol. Chem.* **1995**, *24*, 719.
(50) Inada, Y.; Funahashi, S. *Anal. Sci.* **1997**, *13*, 373.
(51) Inada, Y.; Sugata, T.; Ozutsumi, K.; Funahashi, S. *Inorg. Chem.* **1998**, *37*, 1886.
(52) Storm, C. B.; Teklu, Y. *J. Am. Chem. Soc.* **1972**, *94*, 1745.
(53) Storm, C. B.; Teklu, Y.; Sokoloski, A. *Ann. N.Y. Acad. Sci.* **1973**, *206*, 631.
(54) Momot, K. I.; Walker, F. A. *J. Phys. Chem. A* **1997**, *101*, 9207.
(55) Tan, H.; Simonis, U.; Shokhirev, N. V.; Walker, F. A. *J. Am. Chem. Soc.* **1994**, *116*, 5784.
(56) Berliner, L. J.; Reuben, J. *Biological Magnetic Resonance*; Plenum Press: New York, 1993.
(57) Bertini, I.; Luchinat, C. *NMR of Paramagnetic Molecules in Biological Systems*; Benjamin: California, 1986.

Table 3. Values of Chemical Shift for H_2tpp and the SAT Complex

		δ (relative to TMS)/ppm			
solute	solvent	N−H	phenyl(*o*)	phenyl(*m*,*p*)	pyrrole(β)[a]
H_2tpp	$CDCl_3$	−2.77(s)	7.71−7.78(m)	8.20−8.23(m)	8.84(s)
H_2tpp	CD_3CN	−2.87(s)	7.80−7.87(m)	8.22−8.25(m)	8.85(s)
H_2tpp[b]	$CDCl_3/CS_2$	−3.33(s)	7.8(m)	8.3(m)	8.75(s)
H_2tpp[b,c]	$CDCl_3/CS_2$				8.90(d), 8.61(s)
$Cu(H_2tpp)^{2+}$	CD_3CN	−2.05(s)	7.31−7.50(m)	8.10−8.12(m)	8.66(d), 8.77(s)

[a] When two values are represented, the former is the value of the β-H on the pyrrole groups with N−H proton and the latter is that of the other. [b] Reference 52. [c] At −80 °C.

Chart 1

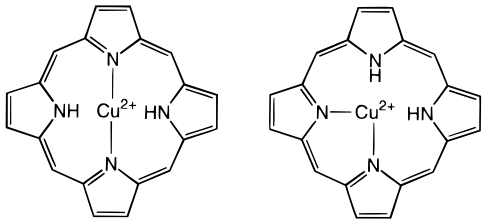

1 **2**

Table 4. Rate Constants[a] for Formation and Deprotonation of the SAT Complex

Formation	
k_{S0}/mol^{-1} dm^3 s^{-1}	$(3.6 \pm 0.1) \times 10^5$
$\Delta H_{S0}^{\ddagger}$/kJ mol^{-1}	56 ± 5
$\Delta S_{S0}^{\ddagger}$/J mol^{-1} K^{-1}	46 ± 19
k_{S1}/mol^{-1} dm^3 s^{-1}	$(3.6 \pm 0.3) \times 10^4$
k_{S2}/mol^{-1} dm^3 s^{-1}	90 ± 2
Deprotonation	
k_{-H1}/mol^{-1} dm^3 s^{-1}	$(2.3 \pm 0.1) \times 10^2$
$k_{-H2}K_{SP}$/mol^{-2} dm^6 s^{-1}	$(5.1 \pm 0.5) \times 10^3$

[a] At 25.0 ± 0.1 °C.

Formation Kinetics of the SAT Complex in Acetonitrile. The conditional first-order rate constants (k_{obs}) for the SAT complex formation were determined under the pseudo-first-order conditions with excess Cu(II) concentration (C_{Cu}) (Table S1) and evaluated to be proportional to C_{Cu} as shown in Figure S5. Thus, k_{obs} values were given as $k_{obs} = k_{S0}C_{Cu}$. The second-order rate constant k_{S0}, the activation enthalpy $\Delta H_{S0}^{\ddagger}$, and the activation entropy $\Delta S_{S0}^{\ddagger}$ for the SAT complex formation were determined to be $(3.6 \pm 0.1) \times 10^5$ mol^{-1} dm^3 s^{-1} at 25.0 ± 0.1 °C, 56 ± 5 kJ mol^{-1}, and 46 ± 19 J mol^{-1} K^{-1}, respectively (Table 4).

Usually, the rates of both solvent exchange and complexation reactions of the Cu(II) ion are extremely fast due to the lability at elongated axial sites. The values of $\Delta H^{\ddagger}$ and $\Delta S^{\ddagger}$ for solvent exchange were respectively reported as 11.5 kJ mol^{-1} and −21.8 J mol^{-1} K^{-1} in H_2O,[58] 24.3 kJ mol^{-1} and 8.1 J mol^{-1} K^{-1} in DMF,[59] and 17.2 kJ mol^{-1} and −44.0 J mol^{-1} K^{-1} in methanol,[60,61] and it has been interpreted that the reaction proceeds via a dissociative-interchange mechanism at a labilized axial site. Although unfortunately the $\Delta H^{\ddagger}$ value in AN has not been available, it is estimated to be 10−20 kJ mol^{-1} by analogy to the trend of $\Delta H^{\ddagger}$ values for the first-row transition metal(II) ions in H_2O, DMF, and methanol.[62] The larger $\Delta H^{\ddagger}$ value of 56 kJ mol^{-1} for the SAT complex formation in comparison with that for the solvent exchange is attributable to the distortion pre-equilibrium of the porphyrin ring. To distort the highly conjugated π-system of the porphyrin ring must require a positive enthalpy change as calculated by Scheidt et al. using molecular mechanics.[63] The distortion pre-equilibrium should also lead to a large positive value of $\Delta S^{\ddagger}$ due to the increase in intramolecular freedom of the stretching and bending modes in the porphyrin ring. Thus, we have concluded that the SAT complex formation is followed by the reaction scheme as follows:

$$H_2tpp \overset{K_D}{\rightleftharpoons} H_2tpp^{\dagger} \quad (5)$$

$$Cu^{2+} + H_2tpp^{\dagger} \overset{K_{OS}}{\rightleftharpoons} Cu^{2+}\cdots H_2tpp^{\dagger} \quad (6)$$

$$Cu^{2+}\cdots H_2tpp^{\dagger} \xrightarrow{k_{ex}} Cu(H_2tpp)^{2+} \quad (7)$$

where K_D and K_{OS} represent the distortion pre-equilibrium constant and the outer-sphere association constant between the distorted H_2tpp ($H_2tpp^{\dagger}$) and Cu^{2+}, respectively. The rate-determining step (reaction 7) is thought to be the exchange with a dissociative-interchange mechanism between a bound AN molecule at the axial site and a pyrrolenine nitrogen of $H_2tpp^{\dagger}$. The succeeding chelate ring closure step to form the SAT complex, in which H_2tpp coordinates to the Cu(II) ion as a bidentate ligand, is generally faster than the coordination of a first donor atom.

Zero intercept of the plot of k_{obs} values as a function of C_{Cu}, as shown in Figure S5, suggests the quantitative formation of the SAT complex, and the overall formation constant can be estimated to be larger than 10^7 mol^{-1} dm^3. As seen in the formation constants of the Cu(II)−py complexes, the larger formation constant of the SAT complex in AN rather than in the other solvents[12,17] is due to the weaker solvation ability of AN for the Cu(II) ion. Furthermore, in comparison with the formation constant of $Cu(py)^{2+}$ ($\beta_1 = 10^{6.4}$ mol^{-1} dm^3), the larger value for the SAT complex formation supports that H_2tpp coordinates to the Cu(II) ion as a bidentate ligand, because the basicity of H_2tpp is smaller than that of py.[64−66] This is consistent with the determination of structure **1** by ^{1}H NMR.

Formation Kinetics of SAT and Cu(tpp) Complexes in the Presence of Pyridine. The spectral changes for the reaction of H_2tpp with the Cu(II)−py complexes in the presence of various amounts of py showed that the reaction product was

(58) Powell, D. H.; Helm, L.; Merbach, A. E. *J. Chem. Phys.* **1991**, *95*, 9258.
(59) Powell, D. H.; Furrer, P.; Pittet, P.-A.; Merbach, A. E. *J. Phys. Chem.* **1995**, *99*, 16622.
(60) Poupko, R.; Luz, Z. *J. Chem. Phys.* **1972**, *57*, 3311.
(61) Helm, L.; Lincoln, S. F.; Merbach, A. E. *Inorg. Chem.* **1986**, *25*, 2550.
(62) Wilkins, R. G. *Kinetics and Mechanism of Reactions of Transition Metal Complexes*; VCH: New York, 1991.
(63) Cheng, B.; Munro, O. Q.; Marques, H. M.; Scheidt, W. R. *J. Am. Chem. Soc.* **1997**, *119*, 10732.
(64) The reported pK_a value of H_3tpp^+ (4.4 in water)[65] is smaller than that of Hpy^+ (5.3 in water).[66] The trend of basicity in AN is usually the same as in water.[25]
(65) Aronoff, S. *J. Phys. Chem.* **1958**, *62*, 428.
(66) Smith, R. M.; Martell, A. E. *Critical Stability Constants*; Plenum Press: New York, 1975.

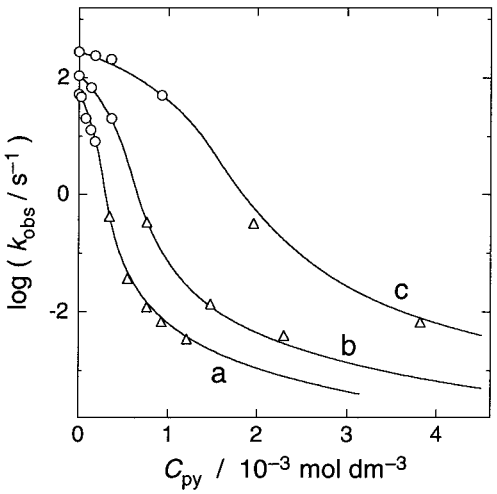

Figure 2. Plots of logarithmic values of conditional first-order rate constants for formation of the SAT complex (circles) and Cu(tpp) (triangles) as a function of C_{py}, where (a) $C_{Cu} = (1.41-1.50) \times 10^{-4}$ mol dm^{-3}, (b) $C_{Cu} = (2.98-3.01) \times 10^{-4}$ mol dm^{-3}, and (c) $C_{Cu} = (7.67-7.79) \times 10^{-4}$ mol dm^{-3}.

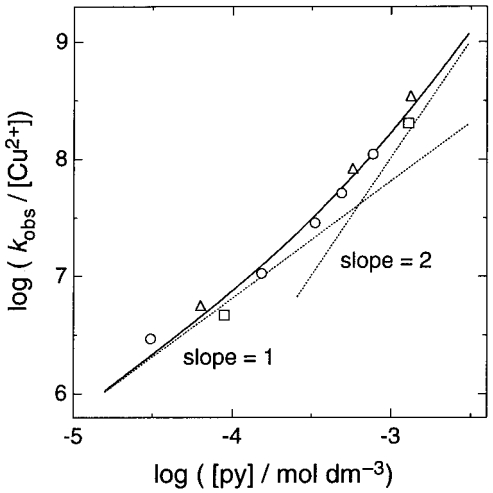

Figure 3. Plot of logarithmic values of k_{obs} for Cu(tpp) formation shown in Figure 2 as a function of log([py]/mol dm^{-3}). Circles, triangles, and squares represent the values at $C_{Cu} = (1.41-1.50) \times 10^{-4}$, $(2.98-3.01) \times 10^{-4}$, and $(7.67-7.79) \times 10^{-4}$ mol dm^{-3}, respectively.

changed from the SAT complex (Figure S6A) to Cu(tpp) (Figure S6B) with increasing C_{py}. It was indicated that Cu(tpp) was not formed until the concentration of free py ([py]) exceeded twice the total concentration of H_2tpp ($[H_2tpp]_0$). This clearly means that a proton acceptor, py in this case, is necessary to form Cu(tpp) in AN. Unobservable formation of the SAT complex in the sample solutions with $[py] \gg 2[H_2tpp]_0$ suggests that the formation constant of the SAT complex with $Cu(py)_n^{2+}$ will be decreased with an increasing number of n. The conditional first-order rate constants (k_{obs}) determined as a function of C_{py} at 25.0 ± 0.1 °C (Table S2) are plotted against C_{py} in the case of three different C_{Cu} in Figure 2.

The change in k_{obs} for the SAT complex formation (circles in Figure 2) was perfectly reproduced by taking into consideration the contribution of $Cu(py)^{2+}$ and $Cu(py)_2^{2+}$ species and no contribution of $Cu(py)_3^{2+}$ and $Cu(py)_4^{2+}$ species, as shown in eqs 8−10.

$$Cu^{2+} + H_2tpp \xrightarrow{k_{S0}} Cu(H_2tpp)^{2+} \quad (8)$$

$$Cu(py)^{2+} + H_2tpp \xrightarrow{k_{S1}} Cu(H_2tpp)(py)_m^{2+} + (1-m)py, \quad m = 0, 1 \quad (9)$$

$$Cu(py)_2^{2+} + H_2tpp \xrightarrow{k_{S2}} Cu(H_2tpp)(py)_n^{2+} + (2-n)py, \quad n = 0-2 \quad (10)$$

Under the present experimental conditions ($[H_2tpp]_0 = 1.5 \times 10^{-6}$ mol dm^{-3}, $C_{Cu} = 1.46$, 2.98, and 7.72×10^{-4} mol dm^{-3}, and $C_{py} = (1.75-14.3) \times 10^{-4}$ mol dm^{-3}), k_{obs} is given by eq 11, because it is acceptable that the formation and dissociation rates of the Cu(II)−py complexes are more rapid than the formation rate of the SAT complex.

$$k_{obs} = k_{S0}[Cu^{2+}] + k_{S1}[Cu(py)^{2+}] + k_{S2}[Cu(py)_2^{2+}] \quad (11)$$

By a least-squares analysis fixing the β_n ($n = 1-4$) and k_{S0} values independently determined, the second-order rate constants were obtained as follows: $k_{S1} = (2.7 \pm 1.1) \times 10^4$ mol^{-1} dm^3 s^{-1} and $k_{S2} = (7 \pm 2) \times 10^3$ mol^{-1} dm^3 s^{-1}.

The k_{obs} values of the Cu(tpp) formation (triangles in Figure 2) also decreased with increasing C_{py}. As shown in Figure 3, the slope of the log−log plot of $k_{obs}/[Cu^{2+}]$ against [py] is varied from 1 to 2. Thus, it can be deduced that the reacting Cu(II) species are $Cu(py)^{2+}$ and $Cu(py)_2^{2+}$. The reactions to form Cu(tpp) are then expressed as reactions 12 and 13, and k_{obs} values were analyzed using eq 14.

$$Cu(py)^{2+} + H_2tpp \xrightarrow[py]{k_{S1}'} Cu(tpp) + 2Hpy^+ \quad (12)$$

$$Cu(py)_2^{2+} + H_2tpp \xrightarrow[py]{k_{S2}'} Cu(tpp) + 2Hpy^+ \quad (13)$$

$$k_{obs} = k_{S1}'[Cu(py)^{2+}] + k_{S2}'[Cu(py)_2^{2+}] \quad (14)$$

Under the experimental conditions where the Cu(tpp) formation occurs, the contribution of Cu^{2+} is negligible because of its extremely small concentration. It is reasonable that the protons released by reactions 12 and 13 will be stabilized by the coexisting py. The rate constants were determined as follows: $k_{S1}' = (2.6 \pm 0.8) \times 10^4$ mol^{-1} dm^3 s^{-1} and $k_{S2}' = (1.3 \pm 0.6) \times 10^2$ mol^{-1} dm^3 s^{-1}. The finding that the values of k_{S1} and k_{S2} are almost identical to those of k_{S1}' and k_{S2}', respectively, indicates that the SAT complexes should be formed in the process of the Cu(tpp) formation and that the SAT complex formation should be a rate-determining step for the Cu(tpp) formation, because k_{S1}' and k_{S2}' might be much smaller than k_{S1} and k_{S2}, respectively, if the SAT complex formation is a pre-equilibrium state prior to a rate-determining deprotonation. This conclusion was also supported by the results of the deprotonation rates of the SAT complex (vide infra). Using all points in Figure 2 according to eq 11, the values of k_{S1} and k_{S2} were finally determined to be $(3.6 \pm 0.3) \times 10^4$ mol^{-1} dm^3 s^{-1} and 90 ± 2 mol^{-1} dm^3 s^{-1} at 25.0 ± 0.1 °C, respectively (Table 4). The calculated curves in Figure 2 reproduce very well the experimental k_{obs} values over the whole range of C_{py}.

It should be noted that the rate constant of the SAT complex formation gradually decreases with an increasing number of py molecules coordinating to the Cu(II) ion, $k_{S0} > k_{S1} > k_{S2}$, though the $Cu-N(an)_{eq}$ bond length becomes longer with respect to the number of py molecules around the Cu(II) ion (vide supra). It has been known that the exchange of a bound solvent is labilized by the coordination of an electron donor to the metal

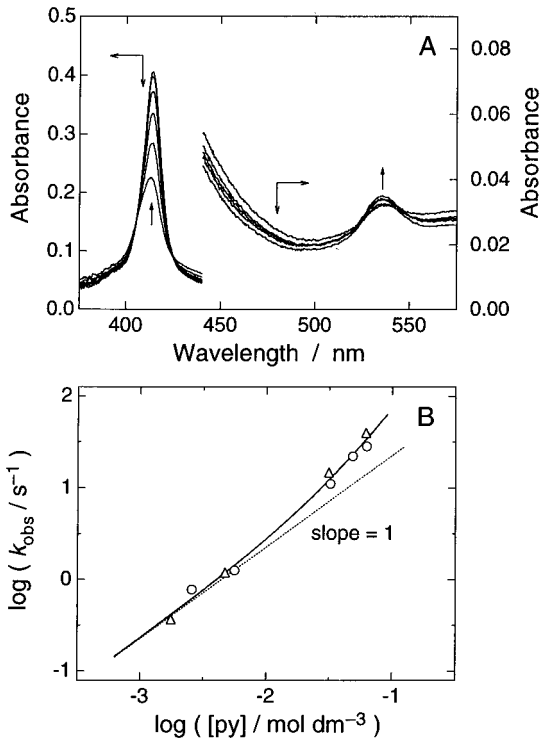

Figure 4. Absorption spectral change during the deprotonation of the SAT complex by pyridine in acetonitrile (A) and the log−log plot of conditional first-order rate constants of the deprotonation against [py] (B). In (B), circles and triangles respresent k_{obs} values at $C_{Cu} = 1.94 \times 10^{-4}$ and 4.41×10^{-4} mol dm^{-3}, respectively.

center.[67−70] The trend in rates of SAT complex formation with Cu^{2+}, $Cu(py)^{2+}$, and $Cu(py)_2^{2+}$ is opposite to the expectation from the change in the Cu−$N(an)_{eq}$ bond length and the electron donation by the coordinating py. The solvent exchange on the Jahn−Teller distorted Cu(II) ion proceeds with the fast intramolecular axial−equatorial (ax/eq) interconversion, and at that time, all three N(an)−Cu−N(an) axes can interconvert.[58−61] For $Cu(py)^{2+}$ with an unsymmetrical coordination sphere, the ax/eq interconversion is limited only for two N(an)−Cu−N(an) axes. In the case of $Cu(py)_2^{2+}$, in which the py molecules are reasonably coordinated in cis geometry, the exchange of AN molecules in equatorial sites is thought to proceed by direct exchange with the AN molecules in the second coordination sphere, because interconversion is impossible, and thus the rate should be much slower. The decrease in the rate constants of the SAT complex formation can be interpreted by a decrease in the frequency of the ax/eq interconversion. This is the first report of the systematic determination of the rates for the complexation of a series of Cu(II) species.

Deprotonation Kinetics of the SAT Complex. For the overall metalation process of H_2tpp, the release of the N−H protons is required for its completion. Figure 4A shows the spectral change in the reaction between the SAT complex and py. Because the regeneration of free H_2tpp by the addition of py was not observed during the course of the reaction, py directly reacted with the SAT complex. There were clear isosbestic points at 405 and 425 nm, and the absorbance change at 414 nm was first order with respect to the SAT complex. The final spectrum was perfectly identical to that of the independently prepared Cu(tpp), which was characterized by a specific absorption peak of Cu(tpp) at 535 nm. The values of $\log(k_{obs}/s^{-1})$ for the deprotonation of the SAT complex (Table S3) are then plotted against log([py]/mol dm^{-3}) in Figure 4B. The slope of the plot is changed from 1 to 2. The k_{obs} values have been analyzed using eq 15 derived according to the reaction scheme of eqs 16−19,

$$k_{obs} = k_{-H1}[py] + k_{-H2}K_{SP}[py]^2 \quad (15)$$

$$Cu(H_2tpp)^{2+} + py \overset{K_{SP}}{\rightleftharpoons} Cu(py)(H_2tpp)^{2+} \quad (16)$$

$$Cu(H_2tpp)^{2+} + py \xrightarrow{k_{-H1}} Cu(Htpp)^{+} + Hpy^{+} \quad (17)$$

$$Cu(py)(H_2tpp)^{2+} + py \xrightarrow{k_{-H2}} Cu(py)_m(Htpp)^{+} + Hpy^{+} + (1-m)\,py, \quad m = 0, 1 \quad (18)$$

$$Cu(py)_m(Htpp)^{+} + py \xrightarrow{fast} Cu(tpp) + Hpy^{+} + m\,py, \quad m = 0, 1 \quad (19)$$

where K_{SP} is the equilibrium constant for binding of py to the Cu(II) ion in the SAT complex, and k_{-H1} and k_{-H2} are the second-order rate constants for the deprotonation of pyrrole protons in $Cu(H_2tpp)^{2+}$ and $Cu(py)(H_2tpp)^{2+}$, respectively. The contribution of the other Cu(II)−py complexes can be ruled out by the independence of k_{obs} from C_{Cu}. Because the plot of k_{obs} against [py] was through the origin, we could also ignore a reaction pathway of the self-deprotonation of the SAT complex. This finding was consistent with the results obtained in pure AN. The kinetic parameters at 25.0 ± 0.1 °C were then obtained as follows: $k_{-H1} = (2.3 \pm 0.1) \times 10^2$ mol^{-1} dm^3 s^{-1} and $k_{-H2}K_{SP} = (5.1 \pm 0.5) \times 10^3$ mol^{-2} dm^6 s^{-1} (Table 4). In effect, the conditional rate evaluated using these parameters exceeds the conditional rate for the Cu(tpp) formation between H_2tpp and the Cu(II)−py complexes in the presence of py. This fact strongly supports that the SAT complex formation is the rate-determining step in the overall metalation process. The report that there is no isotope effect on the rates for the metalation of H_2tpp and D_2tpp with the Zn(II) ion in DMF[71] is consistent with the present conclusion.

The overall deprotonation of the SAT complex may be separated into two steps corresponding to the stepwise proton dissociations (eqs 20 and 21).

$$Cu(H_2tpp)^{2+} + py \rightleftarrows Cu(Htpp)^{+} + Hpy^{+} \quad (20)$$

$$Cu(Htpp)^{+} + py \rightleftarrows Cu(tpp) + Hpy^{+} \quad (21)$$

The deprotonation reaction of the anticipated intermediate, $Cu(Htpp)^{+}$, is considered to be faster than that of $Cu(H_2tpp)^{2+}$, because the distance between the central copper and a remaining pyrrole nitrogen with a proton in $Cu(Htpp)^{+}$ must be shorter than those in $Cu(H_2tpp)^{2+}$. If the first deprotonation (reaction 20) is a pre-equilibrium state prior to a rate-determining second deprotonation (reaction 21), the apparent absorbance change for deprotonation must not show first-order kinetic behavior. The present results then indicate that the first deprotonation is a rate-determining step for the overall deprotonation.

The deprotonation can also be observed in the presence of other bases, such as 4-phenylpyridine (pK_a of its conjugate acid

(67) Hioki, A.; Funahashi, S.; Tanaka, M. *Inorg. Chem.* **1986**, *25*, 2904.
(68) Ishii, M.; Funahashi, S.; Tanaka, M. *Inorg. Chem.* **1988**, *27*, 3192.
(69) Mizuno, M.; Funahashi, S.; Nakasuka, N.; Tanaka, M. *Inorg. Chem.* **1991**, *30*, 1550.
(70) Cusanelli, A.; Frey, U.; Richens, D. T.; Merbach, A. E. *J. Am. Chem. Soc.* **1996**, *118*, 5265 and references therein.
(71) Lavallee, D. K.; Onady, G. M. *Inorg. Chem.* **1981**, *20*, 907.

in water = 5.49), 3-hydroxypyridine (pK_a = 5.23), and isoquinoline (pK_a = 5.40) but cannot be observed in the case of a weaker base such as pyrazine (pK_a = 0.97).[72] It should be noted that, because water can act as a base, proton abstraction was observed in the presence of a large amount of water (pK_a = −1.74) over 0.1 mol dm^{-3}. According to our preliminary experiments, the deprotonation rates corresponding to k_{-H1} in the case of py were dependent on the Brønsted basicity of the bases, i.e., the rate was on the order of 4-phenylpyridine ≈ isoquinoline > py > 3-hydroxypyridine ≫ pyrazine > water.

Metalloporphyrin Formation Mechanism. We can generally describe the mechanisms of metalloporphyrin formation on the basis of the present crucial results obtained in AN, together with the previously reported results for a variety of metal ions and porphyrins. The resolvable elementary reactions during the metalation processes of a general porphyrin (H_2p) with a hexasolvated divalent metal ion in a usual donating solvent (S) are summarily expressed by the distortion of the porphyrin ring (eq 22), the outer-sphere encounter formation (eq 23), the exchange of a bound solvent molecule with a first pyrrolenine nitrogen (eq 24), the chelate ring closure to form the SAT complex (eq 25), the first deprotonation of the pyrrole nitrogen in the SAT complex (eq 26), and the second deprotonation to form a metalloporphyrin (eq 27).

$$H_2p \underset{k_{-D}}{\overset{k_D}{\rightleftharpoons}} H_2p^{\dagger}, \quad K_D = \frac{k_D}{k_{-D}} \tag{22}$$

$$MS_6^{2+} + H_2p^{\dagger} \underset{k_{-OS}}{\overset{k_{OS}}{\rightleftharpoons}} MS_6^{2+}\cdots H_2p^{\dagger}, \quad K_{OS} = \frac{k_{OS}}{k_{-OS}} \tag{23}$$

$$MS_6^{2+}\cdots H_2p^{\dagger} \underset{k_{-SAT}}{\overset{k_{SAT}}{\rightleftharpoons}} MS_5(H_2p)^{2+} + S \tag{24}$$

$$MS_5(H_2p)^{2+} \underset{k_{-RC}}{\overset{k_{RC}}{\rightleftharpoons}} MS_4(H_2p)^{2+} + S, \quad K_{RC} = \frac{k_{RC}}{k_{-RC}} \tag{25}$$

$$MS_4(H_2p)^{2+} + S^* \underset{k_{H1}}{\overset{k_{-H1}}{\rightleftharpoons}} MS_3(Hp)^{+} + HS^{*+} + S, \quad K_{-H1} = \frac{k_{-H1}}{k_{H1}} \tag{26}$$

$$MS_3(Hp)^{+} + S^* \underset{k_{H2}}{\overset{k_{-H2}}{\rightleftharpoons}} M(p) + HS^{*+} + 3S, \quad K_{-H2} = \frac{k_{-H2}}{k_{H2}} \tag{27}$$

The value of k_D is reported to be 4.6×10^7 s^{-1} at 25 °C for 5,10,15,20-tetrakis(4-*N*-methylpyridyl)porphyrin in water,[73] and the pathway of k_{OS} is accepted to be diffusion-controlled. Furthermore, the k_{RC} step is generally considered to be faster than the coordination of a first donor atom (k_{SAT}). The present results indicate that the k_{SAT} path is a rate-determining step for the metalation process in the presence of py as a proton acceptor in AN. According to reactions 22−27, the forward and backward rates for reaction 1 (R_f and R_b) are described by eqs 28 and 29, respectively.

$$R_f = K_D K_{OS} k_{SAT} [MS_6^{2+}][H_2p] \tag{28}$$

$$R_b = K_{-H2}^{-1} K_{-H1}^{-1} K_{RC}^{-1} k_{-SAT} [HS^+]^2 [M(p)] \tag{29}$$

These expressions for the metalation and demetalation rates can explain some previously observed trends as follows: (1) the parallel dependence of the metalation rate on the solvent exchange rate and the lability of a bound solvent due to the k_{SAT} step;[13,15,18,19,74−77] (2) the acceleration of the metalation rate for the nonplanar porphyrins due to the K_D step;[10,12−15,78−81] (3) the dependence of the metalation rate on the Brønsted basicity of porphyrins due to the k_{SAT} step;[14,82,83] (4) the $[H^+]^2$-dependent rate law for the demetalation due to the K_{H1} and K_{H2} steps;[84−86] (5) the dependence of the metalation rate of the charged porphyrins on the ionic strength due to the K_{OS} step.[87] However, the pathway such as the second order with respect to metal ion concentration found in DMF[12] and acetic acid[16] for metalation of H_2tpp is not involved. The formation and deprotonation kinetics of the SAT complex, obtained by the strategic use of AN as a solvent with very weak basicity, have been independently first demonstrated in this work, and we have unified the reaction scheme for the overall metalation of the porphyrin.

Acknowledgment. This work was supported by the Grants-in-Aid for Scientific Research (Nos. 09874131, 10440221, 10740305, and 10874081) from the Ministry of Education, Science, Sports and Culture of Japan and the Kurata Research Grant from the Kurata Foundation. The EXAFS measurements were performed under the approval of the Photon Factory Program Advisory Committee (Proposal Nos. 96G004 and 97G054).

Supporting Information Available: Conditional first-order rate constants for the SAT complex formation in AN (Table S1), for the formation of the SAT complex and Cu(tpp) in the presence of py (Table S2), and for the deprotonation of the SAT complex (Table S3); the titration curves and absorption spectra (Figure S1) for the complexation reactions of the Cu(II) ion with py in AN, the observed EXAFS oscillations (Figure S2), the Fourier transform magnitude (Figure S3), the Fourier-filtered and calculated EXAFS oscillations (Figure S4), the k_{obs} values for the SAT complex formation as a function of C_{Cu} (Figure S5), and the changes in absorption spectra corresponding to formation of the SAT complex and Cu(tpp) in the presence of py (Figure S6) (8 pages). Ordering information is given on any current masthead page.

IC980420D

(72) Pettit, L. D.; Powell, K. J. *IUPAC Stability Constants Database SC-Database for Windows*, release 3; IUPAC and Academic Software: U.K., 1997.
(73) Pasternack, R. F.; Sutin, N.; Turner, D. H. *J. Am. Chem. Soc.* **1976**, *98*, 1908.
(74) Choi, E. I.; Fleischer, E. B. *Inorg. Chem.* **1963**, *2*, 94.
(75) Fleischer, E. B.; Choi, E. I.; Hambright, P.; Stone, A. *Inorg. Chem.* **1964**, *3*, 1284.
(76) Kingham, D. J.; Brisbin, D. A. *Inorg. Chem.* **1970**, *9*, 2034.
(77) Tabata, M.; Tanaka, M. *Inorg. Chem.* **1988**, *27*, 203.
(78) Shah, B.; Shears, B.; Hambright, P. *Inorg. Chem.* **1971**, *10*, 1828.
(79) Funahashi, S.; Ito, Y.; Kakito, H.; Inamo, M.; Hamada, Y.; Tanaka, M. *Mikrochim. Acta, Wien I* **1986**, 33.
(80) Shimizu, Y.; Taniguchi, K.; Inada, Y.; Funahashi, S.; Tsuda, Y.; Ito, Y.; Inamo, M.; Tanaka, M. *Bull. Chem. Soc. Jpn.* **1992**, *65*, 771.
(81) Aizawa, S.; Tsuda, Y.; Ito, Y.; Hatano, K.; Funahashi, S. *Inorg. Chem.* **1993**, *32*, 1119.
(82) Reid, J. B.; Hambright, P. *Inorg. Chem.* **1977**, *16*, 968.
(83) Shamim, A.; Hambright, P. *Inorg. Chem.* **1980**, *19*, 564.
(84) Shears, B.; Shah, B.; Hambright, P. *J. Am. Chem. Soc.* **1971**, *93*, 776.
(85) Rahimi, R.; Sutter, T. P. G.; Hambright, P. *J. Coord. Chem.* **1995**, *34*, 283.
(86) Tabata, M.; Oshita, K.; Tanaka, M. *Mikrochim. Acta, Wien I* **1985**, 397.
(87) Nwaeme, J.; Hambright, P. *Inorg. Chem.* **1984**, *23*, 1990.